NASA Technical Memorandum 101035

Estimating the Signal-to-Noise Ratio of AVIRIS Data

Paul J. Curran and Jennifer L. Dungan

November 1988

National Aeronautics and
Space Administration

NASA Technical Memorandum 101035

Estimating the Signal-to-Noise Ratio of AVIRIS Data

Paul J. Curran, Ames Research Center, Moffett Field, California
Jennifer L. Dungan, TGS Technology, Inc., Moffett Field, California

November 1988

National Aeronautics and
Space Administration

Ames Research Center
Moffett Field, California 94035

SUMMARY

To make the best use of narrowband airborne visible/infrared imaging spectrometer (AVIRIS) data, an investigator needs to know the ratio of signal to random variability or "noise" (signal-to-noise ratio or SNR). The signal is land cover dependent and varies with both wavelength and atmospheric absorption and random noise comprises sensor noise and intrapixel variability (i.e., variability within a pixel). The three existing methods for estimating the SNR are inadequate, since typical "laboratory" methods inflate while "dark current" and "image" methods deflate the SNR.

We propose a new procedure called the "geostatistical" method. It is based on the removal of periodic noise by "notch filtering" in the frequency domain and the isolation of sensor noise and intrapixel variability using the semi-variogram. This procedure was applied easily and successfully to five sets of AVIRIS data from the 1987 flying season and could be applied to remotely sensed data from broadband sensors.

1. INTRODUCTION

Optical remote sensing has traditionally relied on the use of imaging sensors, with a few spectrally noncontiguous broad wavebands, to characterize the major peaks and troughs of an object's reflectance spectrum. Such sensors cannot record the diagnostic narrow waveband absorption features that are the basis of identification in laboratory-based spectroscopy. This has led to the development of the imaging spectrometer which registers many narrow waveband images of a scene and enables the creation of a contiguous reflectance spectrum for each pixel in that scene [1], [2]. Leadership in imaging spectrometry for civil environmental applications has been provided by NASA's Jet Propulsion Laboratory (JPL). Their first sensor, the airborne imaging spectrometer (AIS), could sense in 128 near-infrared wavebands with a 365 to 787 m swath and was operational from 1984 to 1986 inclusive [3]. Their second sensor, the airborne visible/infrared imaging spectrometer (AVIRIS) effectively senses in 209 visible and near-infrared wavebands with an 11-km swath [4]-[6]. AVIRIS underwent performance evaluation flights in 1987 [7] and 1988 and will be flying operationally from 1989 onwards.

To optimize the use of AVIRIS data the random variability or "noise" associated with the sensor's signal should be measured. This information is required by every investigator, as noise determines the accuracy with which absorption features can be distinguished in the spectra [8] and objects can be detected on the ground [9]. For instance, an investigator wishing to use AVIRIS data to estimate the biochemical composition of a vegetation canopy will be looking for diagnostic absorption features at a range of wavelengths, including 1.69 μm for lignin, 2.10 μm for starch, and 2.18 μm for protein [10]-[12]. The detection of an absorption feature requires a level of noise that is around an order of magnitude smaller than the absorption depth [8]. Therefore, information on noise is required with each spectrum, if only to determine if detection of a particular absorption feature is possible. Information on noise alone is not very useful, as a given level of noise will have a more deleterious effect on data quality if the signal is low. Therefore, the signal-to-noise ratio (SNR) which can be estimated by the ratio of the signal's mean ($\bar{z}$) to its standard deviation (s), will be used here (Table I).

The major part of the noise in the AVIRIS signal is additive to a signal [13] that decreases sharply with both an increase in wavelength and atmospheric absorption [14], [15]. The aim of the work reported here was to develop a procedure for estimating this wavelength-dependent SNR.

II. ESTIMATING THE SNR OF AVIRIS DATA

AVIRIS data contain periodic (coherent) sensor noise that can be removed and random noise that cannot. The noise of relevance to the investigator is random noise: the random sensor noise, which is image independent, and intrapixel variability, which is a result of spatially heterogeneous pixel contents and is image dependent. Unfortunately, the three methods commonly used to estimate the SNR of remotely sensed imagery (termed for convenience "laboratory," "dark current" and "image") do not isolate this random noise for the investigator (Table I).

A typical laboratory method uses the $\bar{z}$ and s of a bright homogeneous surface to estimate the SNR for only a few wavebands. The presence of periodic noise will decrease the measured SNR below that relevant to the investigator (see above) but this is more than compensated for by the omission of intrapixel variability and more importantly, by the use of an artificially high signal. When using a laboratory method with a homogeneous surface having a 50% albedo, SNRs of 130, 88, 34, and 18 were reported for AVIRIS wavebands centered at 0.7 μm, 1.0 μm, 1.6 μm, and 2.2 μm respectively [16], [17]. A typical "dark current" method uses variation (e.g., s) in the signal dark currents as a measure of noise. It is not a widely used method although it has been applied to AVIRIS data [18], [19]. Unfortunately, the resultant value includes periodic noise which deflates the SNR below a level which is relevant to the investigator. A typical "image" method uses the $\bar{z}$ and s of four, or more, visually homogeneous pixels as an estimate of the SNR [20], [21]. The resultant value is also deflated below that which is relevant to the investigator, for it includes periodic noise and interpixel variability [22], [23], which even on a visually homogeneous area can be around 2% of $\bar{z}$ [24].

To estimate the SNR of the investigator's data a new procedure is proposed which we have termed the "geostatistical" method.

III. THE GEOSTATISTICAL METHOD FOR ESTIMATING THE SNR

Following the removal of periodic noise, random noise must be estimated free of interpixel variability (Table I). We therefore require an estimate of variability at a pixel; a tool to do this is the semivariogram [25]. This is produced from a transect of pixels where the signal z, at pixel number x along the transect has been extracted at $x = 1, 2, ..., n$. The relation between a pair of pixels, h pixels apart (the lag distance) can be given by the variance of the differences between all such pairs (Glossary). The semi-variance $\gamma(h)$, for pixels at distance h apart is given by half their expectation (E) squared difference, as is discussed by Webster [26],

$$\gamma(h) = 1/2E[z(x_i) - z(x_i + h)]^2 \quad . \tag{1}$$

Within the transect there will be m pairs of observations separated by the same lag, which is estimated by

$$\bar{S}^2 = (1/2m) \sum_{i=1}^{m} [z(x_i) - z(x_i + h)]^2 \quad . \tag{2}$$

$\bar{S}^2$ is an unbiased estimate of the semi-variance, y(h), in the population [26] and is a useful measure of the difference between spatially separate pixels [27]. The larger $\bar{S}^2$ is and therefore $\gamma(h)$, the less similar the pixels will be. The semi-variogram is the function that relates semi-variance to lag (Fig. 1) and is described by Webster [26] and Jupp et al. [27]. Three aspects of the semi-variogram are of interest here: the sill, the asymptotic upperbound value of $\gamma(h)$; the nugget variance (C_0), the limit of $\gamma(h)$ when h approaches 0; and the spatially dependent structural variance (C), the sill minus nugget variance. By definition $\gamma(h) = 0$ when $h = 0$ [28]. In practice the limit of $\gamma(h)$ when h approaches 0 has a positive value because the nugget variance represents variability at scales smaller than a pixel. This phenomenon is a characteristic of the "regularized" semi-variogram calculated for plot rather than point data and is discussed further by Journel and Huijbregts [28].

The key argument upon which the geostatistical method is based is that the nugget variance (Fig. 1) is a sound estimate of the spatially independent noise variance relevant to the investigator. This argument is intuitively acceptable as at the limit of $\gamma(h)$, when h approaches 0, the nugget variance does not have a spatial component (Fig. 1) and is comprised almost entirely of random sensor noise and intrapixel variability. The statistical justification for this argument requires consideration of a one-dimensional model where x is a continuous parameter giving location along a linear transect. The observed signal z(x), comprises both radiance r(x) (assumed to be stationary) and noise n(x) (assumed to be stationary, uncorrelated with r(x) and not autocorrelated):

$$z(x) = r(x) + n(x) \quad . \tag{3}$$

Then, by definition, the expectation E of the squared difference between the signals of two points at a lag of h is the semi-variance $\gamma(h)$ (presented here without the division by two or subscripts for clarity),

$$\gamma[z(h)] = E[z(x) - z(x + h)]^2 \quad . \tag{4}$$

The semi-variance is a function only of sampling lag h if z(x) is stationary, being a sum of two stationary functions. Substituting equation (3) into equation (4):

$$\begin{aligned} E[z(x) - z(x+h)]^2 &= E[r(x) + n(x) - r(x + h) - n(x + h)]^2 \\ &= E[r(x) - r(x+h)] + E[n(x) - n(x+h)] \\ &\quad - 2E[(r(x) - r(x + h))(n(x) - n(x + h))] \quad . \end{aligned} \tag{5}$$

As $E[(r(x) - r(x + h))(n(x) - n(x + h))] = 0$, due to the lack of correlation between radiance and noise, the final term in equation (5) drops out. By definition of the semi-variance:

$$\gamma[z(h)] = \gamma[r(h)] + \gamma[n(h)] \quad , \tag{6}$$

where $\gamma[r(h)]$ and $\gamma[n(h)]$ are the semi-variances of the radiance and noise, respectively. If both the radiance and noise are stationary, they can be written in terms of their variances σ_r^2, σ_n^2 and autocorrelation functions $\rho_r(h)$, $\rho_n(h)$ [29]:

$$\gamma[r(h)] = \sigma_r^2[1 - \rho_r(h)] \quad , \tag{7}$$

$$\gamma[n(h)] = \sigma_n^2[1 - \rho_n(h)] \quad . \tag{8}$$

If noise is not autocorrelated, $\rho_n(h) = 1$ for $h = 0$ and $\rho_n(h) = 0$ for $h > 0$. Therefore,

$$\gamma[n(h)] = \sigma_n^2 \text{ for } h > 0$$
$$= 0 \quad \text{for } h = 0 \ . \tag{9}$$

Taking the limits of equation (9) for the three semi-variances:

$$\lim_{(h\to 0)} \gamma[z(h)] = \lim_{(h\to 0)} \gamma[r(h)] + \lim_{(h\to 0)} \gamma[n(h)]$$

$$= \lim_{(h\to 0)} \sigma_r^2 [1 - \rho_r(h)] + \sigma_n^2 \ . \tag{10}$$

If r(x) were not autocorrelated, the radiance variance σ_r^2 would, when the limit of the semi-variance was $h \to 0$, contaminate the estimate of the noise variance σ_n^2:

$$\lim_{(h\to 0)} \gamma[z(h)] = \sigma_r^2 + \sigma_n^2 \ . \tag{11}$$

However, in practice r(x) is highly autocorrelated for small lags due to the point-spread function of the sensor. Therefore, the contribution of the term containing σ_r^2 is very small in relation to σ_n^2 and the semi-variance of the radiance $\gamma[z(h)]$ at the limit is nearly equal to the noise variance σ_n^2,

$$\lim_{(h\to 0)} \gamma[z(h)] = \sigma_n^2 \ . \tag{12}$$

Accepting equation (12), the square root of the nugget variance can be used to estimate the standard deviation of the random noise and intrapixel variability and thereby the SNR of AVIRIS data,

$$\text{SNR} \simeq \bar{z}/\sqrt{C_0} \ , \tag{13}$$

and as $\bar{z}$ and $\sqrt{C_0}$ have wavelength dependence [25], [30], this calculation should be made for each waveband sensed by AVIRIS.

IV. ASSUMPTIONS IN THE USE OF THE GEOSTATISTICAL METHOD FOR ESTIMATING THE SNR

The two assumptions made in the above derivation (Section III) and three others that are implicit in the use of the geostatistical method are summarized in Table II. Those of stationarity and isotropy are usually acceptable within a land cover. But to check for compliance, transects of AVIRIS spectra can be examined for evidence of a spatial trend or a difference between columns and rows (Fig. 2). In the AVIRIS data discussed in section V there are gain and offset variations (Fig. 2), and so these data are anisotropic. Estimates of the SNR are therefore direction-dependent and either all row or all column transects should be used.

The assumption of a fixed spatial resolution is met with AVIRIS data but could be a problem if the geostatistical method is applied to optical remotely sensed data with a very wide field of view. The assumption that pixels in the scene have spatial dependence and are not randomly ordered is also reasonable. Caution is needed, however, as the very name "nugget variance" was originally used to describe the spatially independent variance in semi-variograms of gold concentration that was due to a random gold nugget at one of the prospector's transect points. Clearly, random scene variability, which could be useful information, cannot be ruled out as a contributor to the nugget variance but it can be minimized by the careful location of transects (Fig. 2). By contrast, the assumption that nugget variance is independent of spatially dependent structural variance at the limit of $\gamma(h)$, when h approaches 0, is unreasonable. This is because of the need to extrapolate from $h = 1$ to the limit of $\gamma(h)$, when h approaches 0, using the spatially dependent slope. Fortunately the point-spread function of the sensor increases the similarity of pixels at small lags and so minimizes the effect of violating this assumption.

V. THE GEOSTATISTICAL METHOD FOR ESTIMATING THE SNR OF AVIRIS DATA

Application of the geostatistical method involved two stages, first, data selection and preprocessing and second, estimation of the SNR for each waveband of AVIRIS data.

Selection and Preprocessing of AVIRIS Data

Five AVIRIS data sets were selected (Table III). They were recorded around solar noon, over a wide range of dates and land covers. All data were converted from digital numbers to radiance and radiometrically calibrated at JPL [31] and on receipt, any dropped scan lines were replaced with the means of radiance values in adjacent lines [32]. The 1987 AVIRIS data contained considerable periodic noise, produced by the inadvertent coupling of the image signal with electrical and mechanical signals [17]. A fast Fourier transform [33], [34] was used to generate frequency domain images for each scene (Fig. 3) and these revealed clear noise spikes [35], [36]. This periodic noise was dominated by frequencies of around two pixels per cycle that increased in severity as the season progressed (Fig. 4). The major periodic noise frequencies were removed by "notch filtering" in the frequency domain [37], [38] by a method (Table IV) similar to that used on AIS data [39]-[41]. By comparison with prefiltered spectra, this removal of major periodic noise had no effect on the relative radiometry (Fig. 5) and by comparison with prefiltered semi-variograms, it reduced the spatially dependent structural variance (C) (Fig. 6). The visual effects of such filtering are illustrated in Fig. 3. The success of this preprocessing was attributed to: (i) clarity of the noise, especially from 0.68 to 1.27 μm (a result of low gain in the second of the four AVIRIS spectrometers) and 1.84-2.40 μm (a result of low signal in the fourth of the four AVIRIS spectrometers) [4]; (ii) clarity of the major periodic noise spikes in the vertical component of the frequency domain; (iii) spectrometer-independence of the major periodic noise frequencies and (iv) relatively homogeneous subscenes with little chance of "ringing" (crenulated tonal boundaries) in the filtered images [39].

Estimating the SNR for Each Waveband of AVIRIS Data

To estimate the SNR for each waveband of AVIRIS data, three transects were first located within each land cover (Table V). These transects were long enough to enable the production of a semi-variogram with at least 15 lags in the statistically significant first fifth of their length [26]. The mean signal and semi-variogram were calculated for each of the 209 wavebands and the nugget variance was determined by extrapolating the slope of the semi-variogram to $h = 0$ (Fig. 1). This extrapolation could have been obtained by the use of an "authorized model" [26] for each semi-variogram. However, to minimize the need for such intensive intervention, the smallest lag at which the sill occurred in the whole

data set was used as a maximum point from which to apply a linear fit to h = 0 (Fig.~1). The results of such extrapolation are illustrated for three wavebands in one data set (Fig. 7). The signal and square root of the nugget variance were used to derive plots of SNR versus wavelength and signal with a noise envelope versus wavelength (Table V, Figs. 8-12). As was noted in the introduction, noise varies little with wavelength but the signal will drop sharply with both an increase in wavelength and atmospheric absorption. As a result the first-order forms of the SNR plots (Figs. 8-12) were signal dependent. The spectral zones of very high SNRs were green/red (0.50-0.70 μm) for water and soil and near-infrared (0.70-0.90 μm) for vegetation. The spectral zones of low and very low SNRs were near-infrared and middle-infrared wavelengths where the signal was low, either at the longer wavelengths or in atmospheric absorption bands (Table VI). These spectral zones of SNR provide a useful summary of the utility of specific AVIRIS wavelengths from the 1987 flight season. Of more importance is the potential use of the geostatistical method by individual investigators to plan for the restrictions that random noise places on the analysis of AVIRIS data.

VI. DISCUSSION

The geostatistical method for estimating the SNR of imagery was proposed and developed in the context of AVIRIS data. The utility of the method is potentially far wider, as it is applicable to any remotely sensed data that can satisfy its rather modest assumptions (Table II). These data include, for example, most optical remotely sensed imagery regardless of altitude of data collection or sensor design. The more general utility of the geostatistical method is to be the topic of future studies.

VII. CONCLUSION

A new procedure, which we have called the geostatistical method, was used to estimate the SNR of five sets of AVIRIS data. This method was designed around the needs of the AVIRIS investigator and has the following advantages: (i) it estimates only noise that is relevant to the investigator, unlike the existing laboratory, dark current and image methods, (ii) it requires acceptable assumptions and (iii) is easy to apply. Future studies will evaluate the utility of this method to remotely sensed data from broad-band sensors.

ACKNOWLEDGEMENTS

This work was funded by the NASA Earth Sciences and Applications Division while PJC held a Senior NRC/NASA Research Associateship at NASA Ames under a grant from the NASA Life Sciences Division. The authors wish to thank Dave Peterson, Nancy Swanberg and Byron Wood (NASA Ames) for their AVIRIS data; Don Card (NASA Ames) for the basis of equations 3-12, and Don Card, Chris Hlavka, Dave Peterson, and Vern Vanderbilt (NASA Ames), Wally Porter and Gregg Vane (NASA JPL), Alex Goetz (University of Colorado), Dave Meyer (EROS Data Center), Peter Atkinson (Sheffield University) and Steve Briggs (NERC) for very helpful discussions.

REFERENCES

[1] A.F.H. Goetz, G. Vane, J.E. Solomon and B.N. Rock, "Imaging spectrometry for Earth remote sensing," Science, vol. 228, pp. 1147-1153, 1985.

[2] G. Vane, "High spectral resolution remote sensing of the Earth," Sensors, pp. 11-19, 1985.

[3] G. Vane and A.F.H. Goetz, "Terrestrial imaging spectrometry," Remote Sensing of Environment, vol. 24, pp. 1-29, 1988.

[4] W.M. Porter and H.T. Enmark, "A system overview of the Airborne Visible/Infrared Imaging Spectrometer (AVIRIS)," in Imaging Spectrometry II, G. Vane, Ed., Society of Photo-Optical Instrumentation Engineers, vol. 834, pp. 22-31, 1987.

] G. Vane, Ed., Airborne Visible/Infrared Imaging Spectrometer AVIRIS. A Description of the Sensor, Ground Data Processing Facility, Laboratory Calibration, and First Results, NASA/JPL Publication 87-38, Pasadena, CA, 1987.

G. Vane, "First results from the Airborne Visible/Infrared Imaging Spectrometer (AVIRIS)," in Imaging Spectrometer II, G. Vane, Ed., Society of Photo-Optical Instrumentation Engineers, vol. 834, pp. 166-174, 1987.

G. Vane, Ed., AVIRIS Performance Evaluation Workshop, NASA/JPL Publication 88-00, (Jet Propulsion Laboratory, Pasadena, CA), in press, 1988.

A.F.H. Goetz and W.M. Calvin, "Imaging spectrometry: spectral resolution and analytical identification of spectral features," in Imaging Spectrometry II, G. Vane, Ed., Society of Photo-Optical Instrumentation Engineers, vol. 834, pp. 158-165, 1987.

P.J. Curran and A.M. Hay, "The importance of measurement error for certain procedures in remote sensing at optical wavelengths," Photogrammetric Engineering and Remote Sensing, vol. 52, pp. 229-241, 1986.

G.C. Marten, J.S. Shenk, and F.E. Barton, Eds., Near Infrared Reflectance Spectroscopy (NIRS): Analysis of Forage Quality, Agriculture Handbook 643, USDA, Washington, DC, 1985.

D. L. Peterson, J.D. Aber, P.A. Matson, D. H. Card, N. Swanberg, C.A. Wessman, and M. Spanner, "Remote sensing of forest canopy and leaf biochemical contents," Remote Sensing of Environment, vol. 24, pp. 85-108, 1988.

C.A. Wessman, J.D. Aber, D.L. Peterson, and J.M. Melillo, "Remote sensing of canopy chemistry and nitrogen cycling in temperature forest ecosystems," Nature, vol. 335, pp. 154-156, 1988.

D.S. Lowe, "Nonphotographic optical sensors," in Remote Sensing of Environment, J. Lintz and D.S. Simonett, Eds., Reading MA: Addison-Wesley, pp. 155-193, 1976.

K. Ya. Kondratyev, Radiation in the Atmosphere. London: Academic Press,1969.

M.T. Chahine, "Interaction mechanisms within the atmosphere," in Manual of Remote Sensing, (2nd Ed.) R.N. Colwell, Ed., Falls Church, VA: American Society of Photogrammetry, pp. 165-230, 1983.

G. Vane, "Workshop overview and AVIRIS project status," in AVIRIS Performance Evaluation Workshop, G. Vane, Ed., NASA/JPL Publication 88-00 (Jet Propulsion Laboratory, Pasadena, CA), in press, 1988.

V. Porter, "AVIRIS instrument status," in AVIRIS Performance Evaluation Workshop, G. Vane, Ed., NASA/JPL Publication 88-00 (Jet Propulsion Laboratory, Pasadena, CA), in press, 1988.

M. Abrams and V. Carerre, "An assessment of AVIRIS spectra acquired over the Goldfield mining district, Nevada," in AVIRIS Performance Evaluation Workshop, G. Vane, Ed., NASA/JPL Publication 88-00 (Jet Propulsion Laboratory, Pasadena, CA), in press, 1988.

G. Vane and R. Green, "Assessment of AVIRIS inflight performance over the Mountain Pass Carbonatite, California," in AVIRIS Performance Evaluation Workshop, G. Vane, Ed., NASA/JPL Publication 88-00 (Jet Propulsion Laboratory, Pasadena, CA), in press, 1988.

...C. Wrigley, D.H. Card, C.A. Hlavka, J.R. Hall, F.C. Metrtz, and C.A. Archwamety, "Thematic Mapper image quality: registration, noise and resolution," IEEE Transactions on Geoscience and Remote Sensing, vol. GE-22, pp. 263-271, 1984.

[21] M.J. Duggin, H. Sakhavat, and J. Lindsay, "Systematic and random variations in Thematic Mapper digital radiance data," Photogrammetric Engineering and Remote Sensing, vol. 51, pp. 1427-1434, 1985.
[22] J. Conel, R. Green, C. Bruegge, J. Margolis, R. Alley, G. Vane, V. Carerre, P. Slater, and R. Jackson, "AVIRIS :(1) field radiometric and spectral calibration, (2) studies of the atmosphere and surface by model and observational methods," in AVIRIS Performance Evaluation Workshop, G. Vane, Ed., NASA/JPL Publication 88-00 (Jet Propulsion Laboratory, Pasadena, CA), in press, 1988.
[23] R. Clark, "Calibration and evaluation of AVIRIS data," in AVIRIS Performance Evaluation Workshop, G. Vane, Ed., NASA/JPL Publication 88-00 (Jet Propulsion Laboratory, Pasadena, CA), in press, 1988.
[24] J.E. Colonel, R.O. Green, G. Vane, C.J. Bruegge, R.E. Alley, and B.J. Curtiss, "Airborne Imaging Spectrometer-2: radiometric spectral characteristics and comparison of ways to compensate for the atmosphere," in Imaging Spectrometry II, G. Vane, Ed., Society of Photo-Optical Instrumentation Engineers, vol. 834 pp. 140-157, 1987.
[25] P.J. Curran, "The semivariogram in remote sensing: an introduction," Remote Sensing of Environment, vol. 24, pp. 493-507, 1988.
[26] R. Webster, "Quantitative spatial analysis of soil in the field," Advances in Soil Science, vol. 3, pp.1-70, 1985.
[27] D.L.B. Jupp, A.H. Strahler, and C.E. Woodcock, "Autocorrelation and regularization in digital images. I. Basic theory," IEEE Transactions on Geoscience and Remote Sensing, vol. GE 26, pp. 463-473, 1988.
[28] A.G. Journel and C.J. Huijbregts, Mining Geostatistics. London: Academic Press, 1978.
[29] J. Odland, Spatial Autocorrelation. London: Sage, 1988.
[30] J.R. Carr and D.E. Myers, "Application of the theory of regionalized variables to the spatial analysis of Landsat data," in Spatial Information Technologies for Remote Sensing Today and Tomorrow: Ninth William T. Pecora Memorial Symposium (IEEE Computer Society, Los Angeles, CA), pp. 55-61, 1984.
[31] G. Vane, T.G. Chrien, E.A. Miller, and J.H. Reimer, "Spectral and radiometric calibration of the Airborne Visible/Infrared Imaging Spectrometer,"in Imaging Spectrometer II, G. Vane, Ed., Society of Photo-Optical Instrumentation Engineers, vol. 834, pp. 91-105, 1987.
[32] P.M. Mather, Computer Processing of Remotely Sensed Images. An Introduction. New York: John Wiley and Sons, 1987.
[33] E.O. Bringham, The Fast Fourier Transform. Englewood Cliffs, NJ: Prentice Hall, 1974.
[34] R.C. Gonzales and P. Wintz, Digital Image Processing. Reading Mass: Addison-Wesley, 1977.
[35] J.M. Young, Noise Characterisation of Airborne Visible and Infrared Imaging Spectrometer Data, Masters Project, Dept. Electrical Engineering, Univ. of Colorado, Boulder, Colorado.
[36] L. Rowan, J. Crowley, and D. Meyer, "Assessment of AVIRIS inflight performance over the Mountain Pass Carbonatite, California," in AVIRIS Performance Evaluation Workshop, G. Vane, Ed., NASA/JPL Publication 88-00 (Jet Propulsion Laboratory, Pasadena, CA), in press, 1988.
[37] A. Rosenfeld and A.C. Kak, Digital Picture Processing. 2nd Ed., New York: Academic Press, 1982.
[38] J.G. Moik, Digital Processing of Remotely Sensed Images. NASA SP-431,Washington, DC: National Aeronautics and Space Administration, 1980.
[39] C. Hlavka, "Destriping AIS data using Fourier filtering techniques," in Proceedings of the Second Airborne Spectrometer Data Analysis Workshop,G. Vane and A.F.H. Goetz, Eds., NASA/JPL Publication 86-35 (Jet Propulsion Laboratory, Pasadena, CA), pp. 74-80, 1986.
[40] C.V. Price and W.E. Westman, "Toward detecting California shrubland canopy chemistry with AIS data," in Proceedings of the Third Airborne Imaging Spectrometer Data Analysis Workshop, G. Vane, Ed., NASA/JPL Publication 87-30 (Jet Propulsion Laboratory, Pasadena, CA), pp. 91-99, 1987.

[41] N.A. Swanberg and P.A. Matson, "The use of airborne imaging spectrometer data to determine experimentally induced variation in coniferous canopy chemistry," in Proceedings of the Third Airborne Imaging Spectrometer Data Analysis Workshop, G. Vane, Ed., NASA/JPL Publication 87-30 (Jet Propulsion Laboratory, Pasadena, CA), pp. 70-74, 1987.

Table I. Existing methods for estimating the SNR of AVIRIS data showing the level of signal and type of noise to be estimated

Method	Signal level	Type of noise				Estimated SNR in relation to that relevant to investigator	Examples for AVIRIS data
		Periodic	Random				
		Sensor noise	Sensor noise	Intra-pixel variability	Inter-pixel variability		
Laboratory	Artificially high	x	x			Higher	[16], [17]
Dark current	Natural	x	x	x		Lower	[18], [19]
Image	Natural	x	x	x	x	Lower	[22], [23]

Table II. Assumptions in the use of nugget variance as an estimate of random noise (random sensor noise and intrapixel variability) in AVIRIS data

Assumption	Explanation or reason	Comments on assumptions in relation to AVIRIS data collected in 1987
Stationarity	Spatial dependence of pixels is a function of lag and not location.	Generally true within a land cover.
Isotropy	Nugget variance is independent of transect direction.	Untrue, due to gain and offset variability; therefore use row or column transects.
Fixed spatial resolution	Intrapixel variability and therefore nugget variance is dependent upon spatial resolution.	True.
Scene does not contain random information.	Random features in scene increase nugget variance and could be information rather than noise.	Generally true but need to check.
Nugget variance is independent of spatially dependent structural variance	Limit of $\gamma(h)$ when h approaches 0 has minor dependence upon the slope of the semi-variogram.	Untrue, but point-spread function of sensor ensures that $\gamma(h)$ when h approaches 0 is similar to that at small lags and so the effect of this violation is minimal.

Table III. AVIRIS data for which the SNR was estimated

Location	Land cover of interest	Date of data acquisition (1987)	Time of data acquisition (start, hr)
Mountain View, CA	Sediment-laden water	25 June	12:40
Gainesville, FL	Plantation forest	4 July	11:49
Yuba City, CA	Bare soil	30 July	12:49
Metolius, OR	Semi-natural forest	1 August	11:14
Cuprite, NE	Bare soil	14 September	11:14

Table IV. Procedure for removing the major periodic noise in AVIRIS data

1. Select 256 x 256 pixel subscene in one waveband.
2. Use fast Fourier transform to create a frequency domain image; major periodic noise appears as a series of spikes, each representing energy concentration at a specific frequency.
3. Design a "notch filter." Zeroes represent the location of major periodic noise spikes and ones represent the remainder. Multiply by frequency domain image to create a new frequency domain image without major periodic noise spikes.
4. Invert filtered frequency domain image to create spatial domain image with no major periodic noise.
5. Repeat step 4 on selected wavebands from each spectrometer. Define spectrometer-independent notch filter and use to filter all AVIRIS wavebands.

Table V. Procedure for estimating the SNR in AVIRIS data

1. Locate three row transects within a land cover, each transect being 75-100 pixels long to ensure that the statistically significant first fifth of the semi-variogram is at least 15 lags.

2. Calculate the mean signal ($\bar{z}$) and semi-variogram for each waveband.

3. Determine the nugget variance (C_0) by extrapolating the slope of $\gamma(h)$ for each waveband. Here the extrapolation was based on a linear fit over 8 lags (Fig. 7).

4. Plot $\bar{z}/\sqrt{C_0}$ versus wavelength and $\bar{z}$ (with a C_0 envelope) versus wavelength as two representations of the SNR (Figs. 8-12).

Table VI. SNR zones in AVIRIS data, where NIR refers to near-infrared and MIR refers to middle-infrared wavelengths

Relative SNR	Land cover		
	Water	Vegetation	Soil
Very high	Green/red (0.50-0.70 μm)	NIR (0.95-1.10 μm)	Green/red (0.50-0.70 μm)
High	Blue (0.40-0.50 μm)	Green/red (0.50-0.70 μm) NIR (0.85-0.90 μm)	Blue (0.40-0.50 μm) NIR (0.95-1.10 μm)
Medium	NIR (0.70-0.90, 0.95-1.10 μm)	Blue (0.40-0.50 μm) NIR (0.70-0.85, 0.90-0.95 μm)	NIR (0.85-0.90 μm)
Low	NIR (0.90-0.95 μm) MIR (1.15-1.35, 1.50-1.75, 2.00-2.30 μm)	MIR (1.10-1.35, 1.50-1.75, 2.00-2.30 μm)	NIR (0.70-0.85, 0.90-0.95 μm) MIR (1.15-1.35, 1.50-1.75, 2.00-2.30 μm)
Very low	MIR (1.10-1.15, 1.35-1.50, 1.75-2.00, 2.30-2.40 μm	MIR (1.35-1.50, 1.75-2.00, 2.30-2.40 μm)	MIR (1.10-1.15, 1.35-1.50, 1.75-2.00, 2.30-2.40 μm

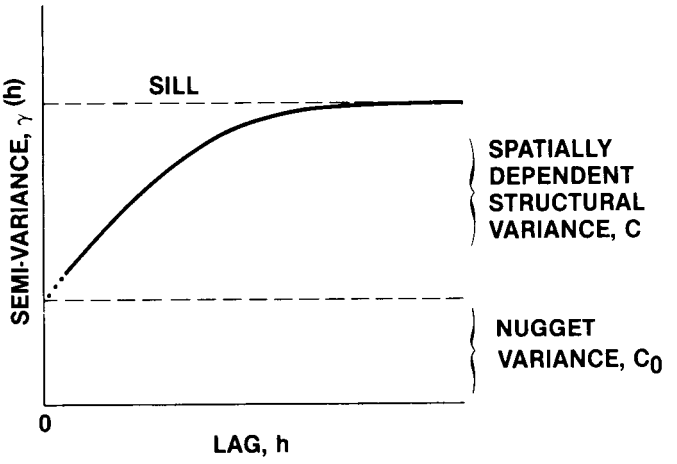

Fig. 1. A generalized semi-variogram.

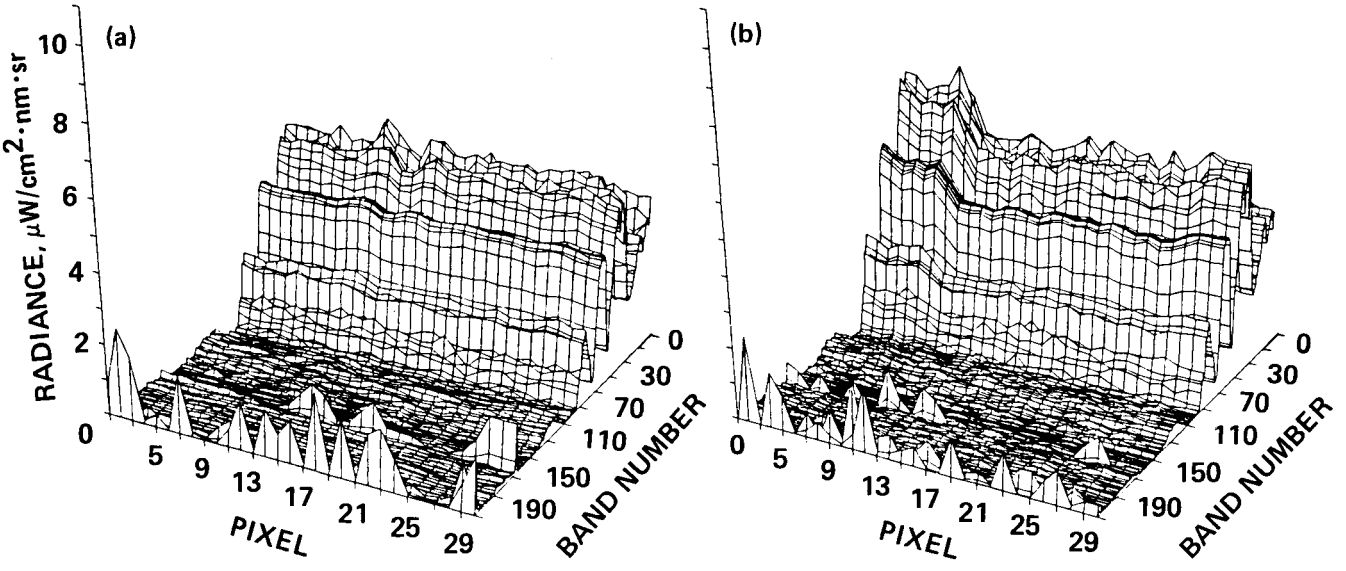

Fig. 2. Two 30-pixel transects for a plantation forest, in the AVIRIS data of Gainesville, FL (Table III), recorded (a) along a row and (b) down a column.

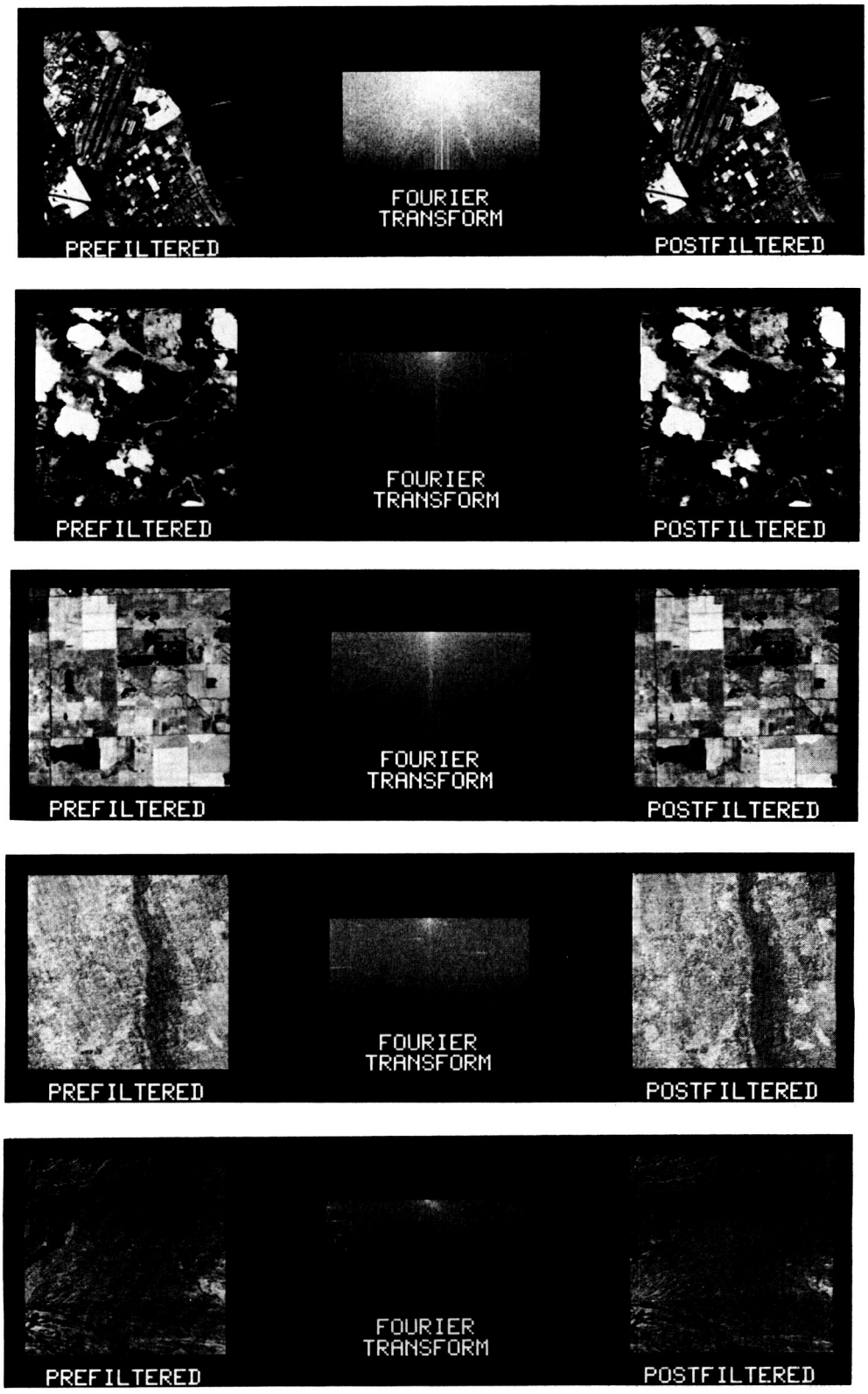

Fig. 3. The removal of major periodic noise by "notch filtering" in the frequency domain of the 1.018 μm waveband of AVIRIS data for: (a) sediment-laden water, Mountain View, CA; (b) plantation forest, Gainesville, FL; (c) bare soil, Yuba City, CA; (d) semi-natural forest, Metolius, OR; and (e) bare soil, Cuprite, NE (Table III).

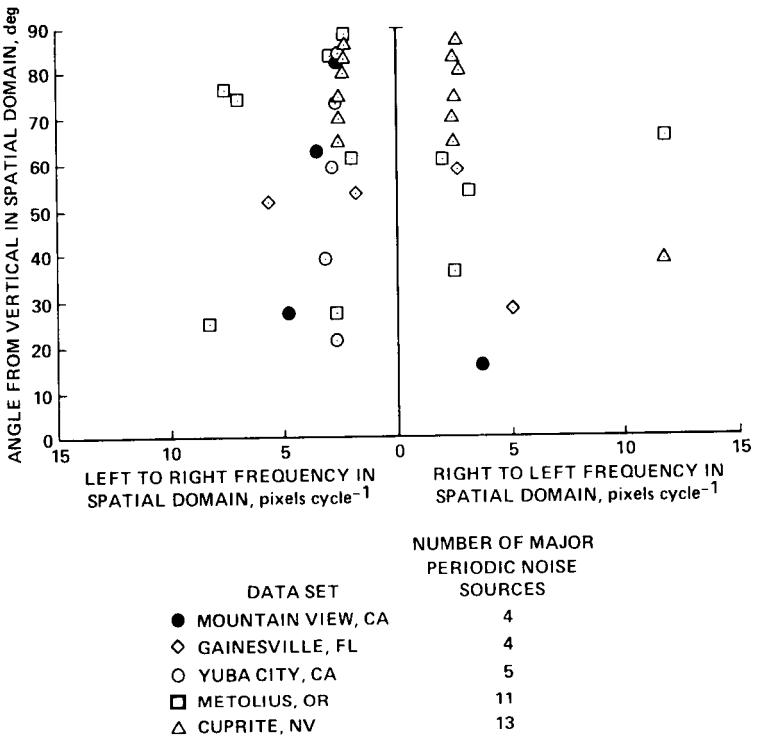

Fig. 4. The major types of periodic noise observed in five sets of AVIRIS data (Table III). The noise characteristics were determined from the location of major periodic noise spikes in the frequency domain.

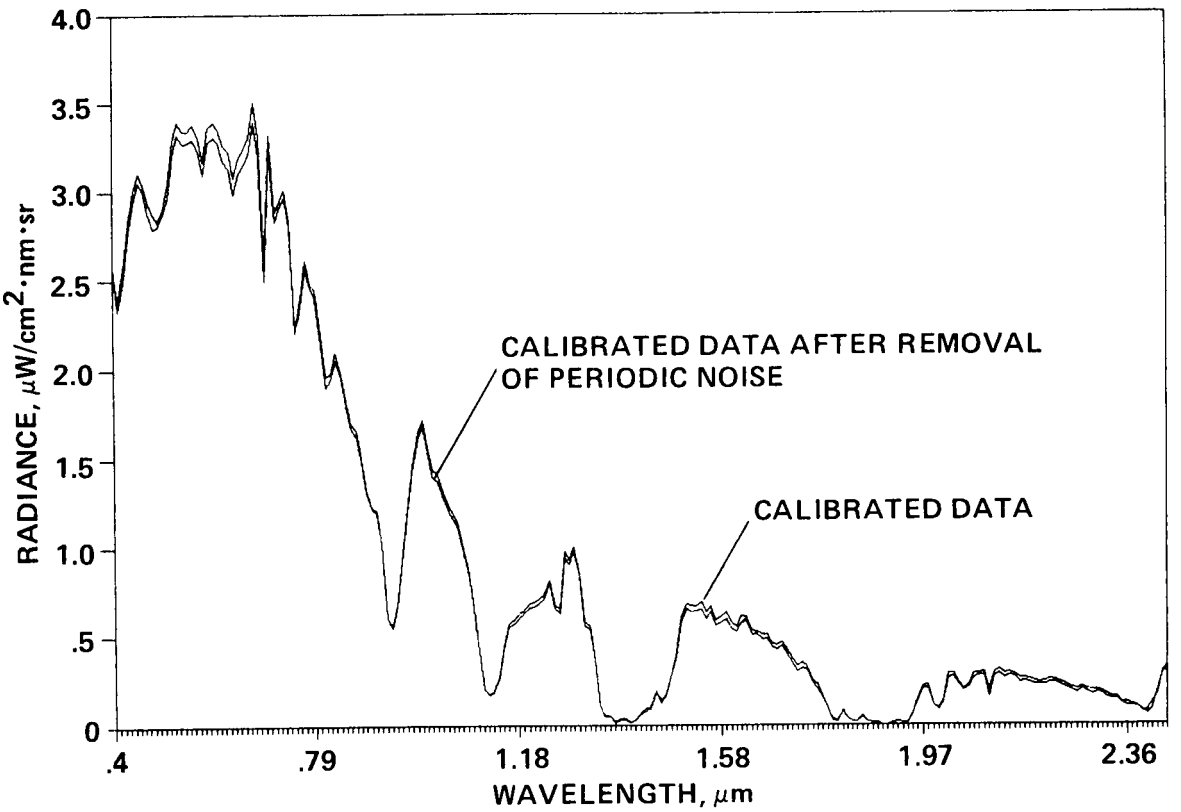

Fig. 5. The effect on a bare soil spectra of removing the major periodic noise by "notch filtering" in the frequency domain. The AVIRIS data are for Cuprite, NE (Table III).

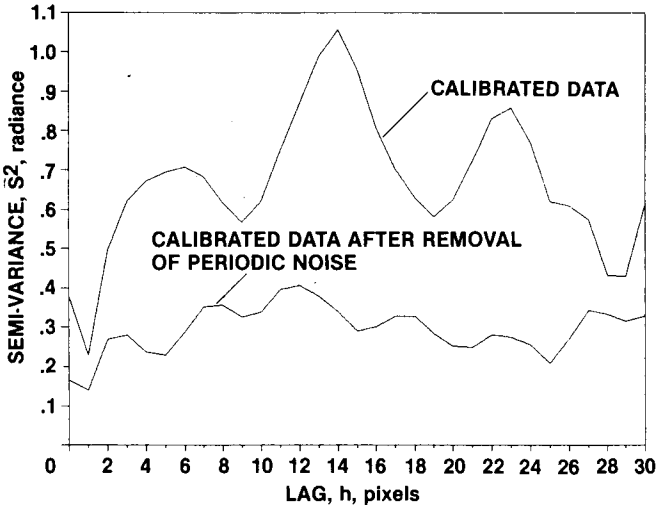

Fig. 6. The effect on a bare soil semi-variogram of removing the major periodic noise by "notch filtering" in the frequency domain. The AVIRIS data are the 1.018 μm waveband for Cuprite, NE (Table III).

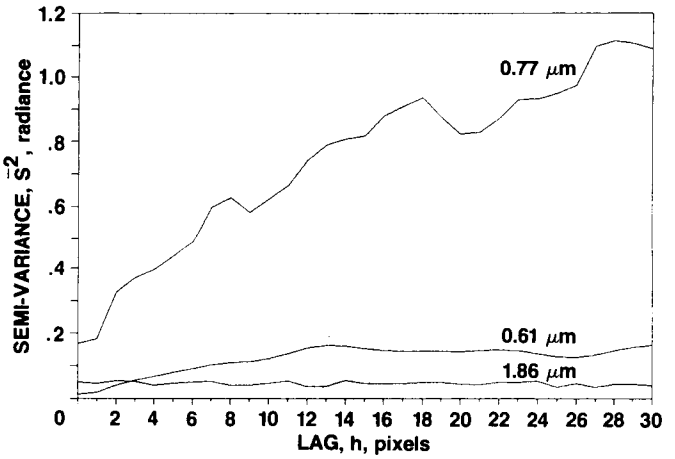

Fig. 7. Semi-variograms for three wavebands of AVIRIS data recorded for a plantation forest near Gainesville, FL (Table III).

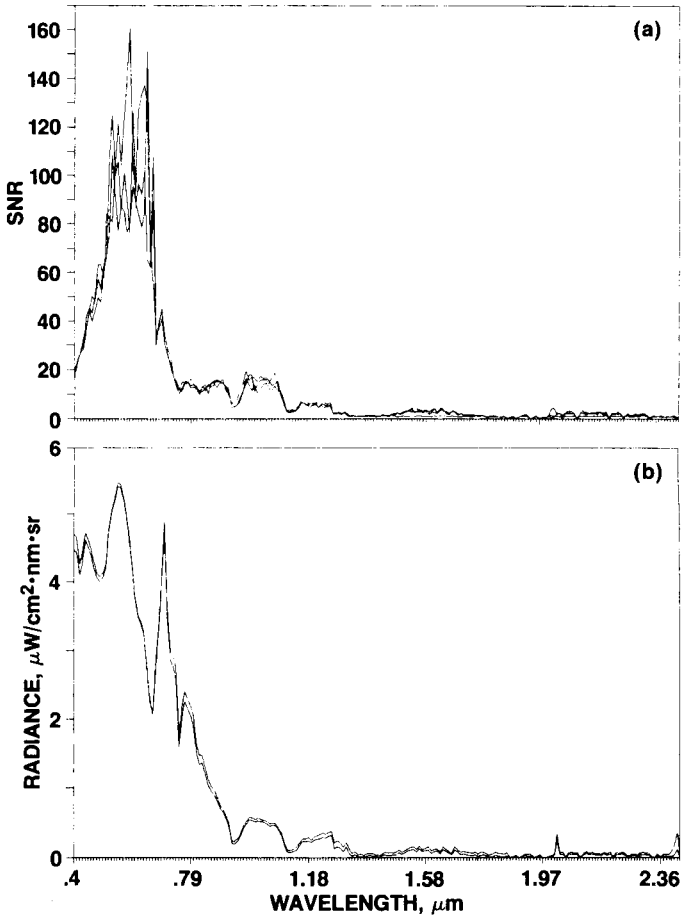

Fig. 8. The SNR for sediment-laden water in the AVIRIS data of Mountain View, CA (Table III): (a) the SNR versus wavelength and (b) the signal with noise envelope versus wavelength for three image transects.

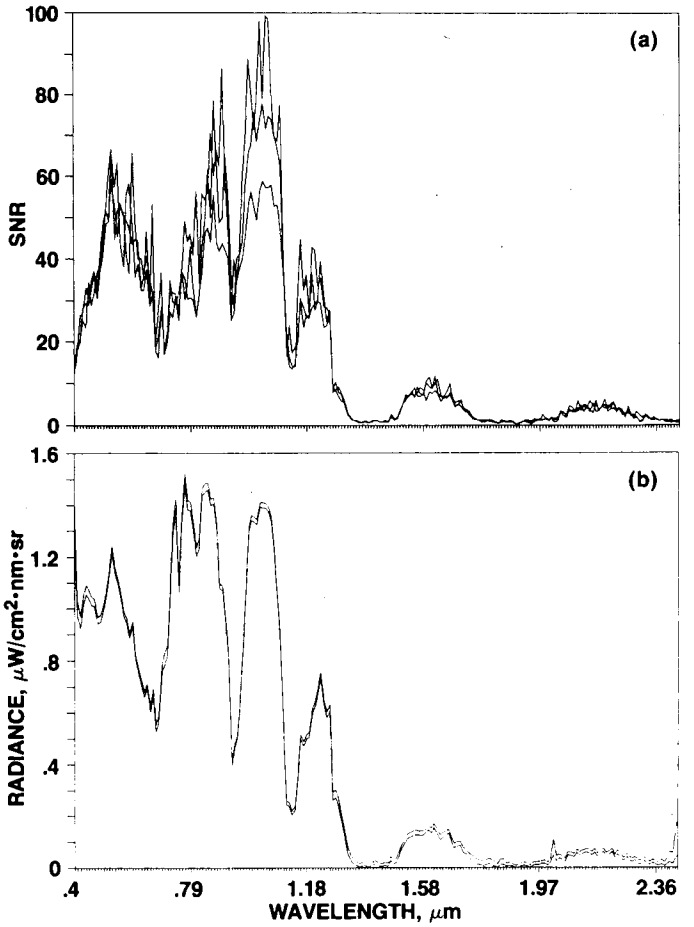

Fig. 9. The SNR for a plantation forest in the AVIRIS data of Gainesville, FL (Table III): (a) the SNR versus wavelength and (b) the signal with noise envelope versus wavelength for three image transects.

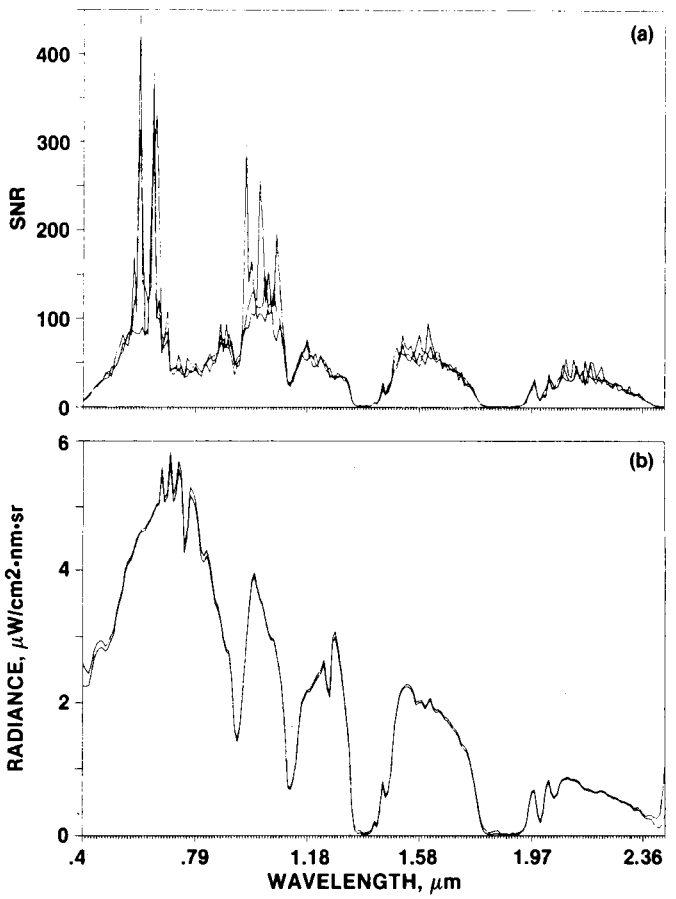

Fig. 10. The SNR for bare soil in the AVIRIS data of Yuba City, CA (Table III): (a) the SNR versus wavelength and (b) the signal with noise envelope versus wavelength for three image transects.

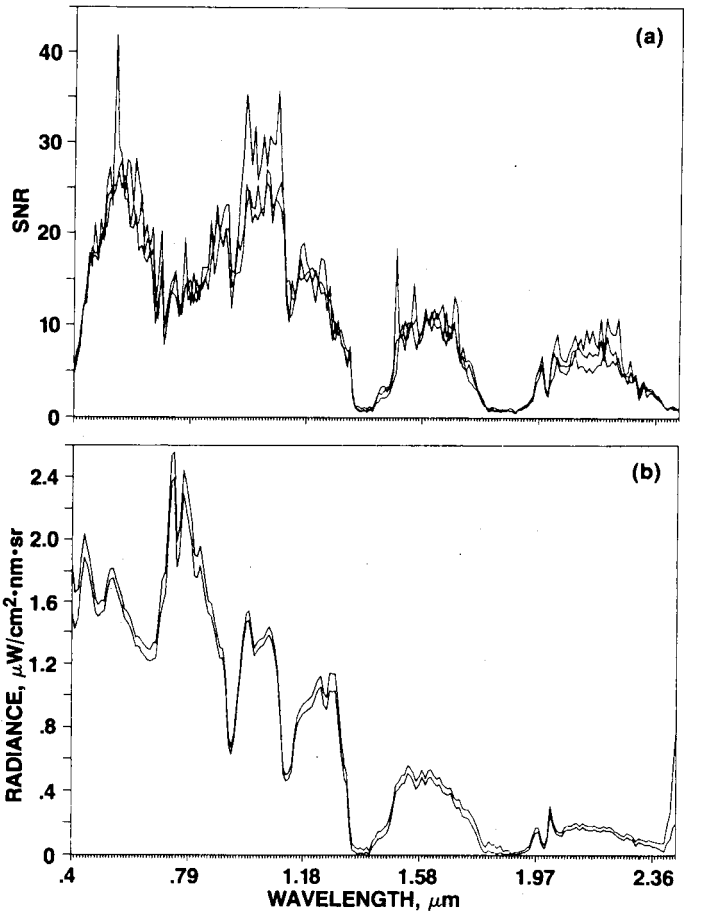

Fig. 11. The SNR for semi-natural forest in the AVIRIS data of Metolius, OR (Table III): (a) the SNR versus wavelength and (b) the signal with noise envelope versus wavelength for three image transects.

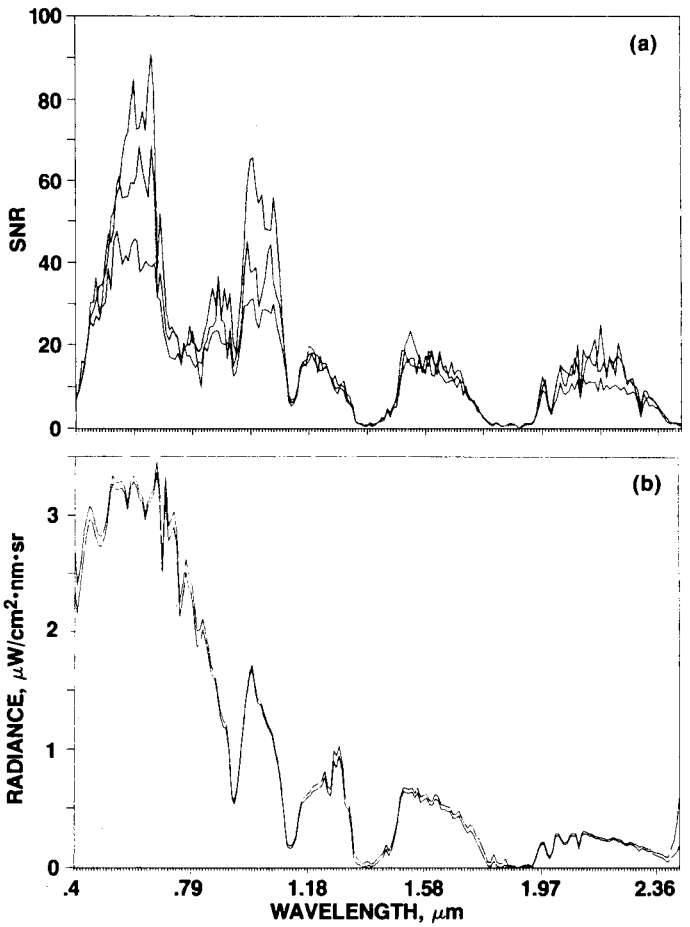

Fig. 12. The SNR for bare soil in the AVIRIS data of Cuprite, NE (Table III): (a) the SNR versus wavelength and (b) the signal with noise envelope versus wavelength for three image transects.

NASA
National Aeronautics and Space Administration

Report Documentation Page

1. Report No.	2. Government Accession No.	3. Recipient's Catalog No.
NASA TM-101035		

4. Title and Subtitle	5. Report Date
Estimating the Signal-to-Noise Ratio of AVIRIS Data	November 1988
	6. Performing Organization Code

7. Author(s)	8. Performing Organization Report No.
Paul J. Curran and Jennifer L. Dungan (TGS Technology, Inc., Moffett Field, CA 94035)	A-88298
	10. Work Unit No. 677-21-35

9. Performing Organization Name and Address	11. Contract or Grant No.
Ames Research Center Moffett Field, CA 94035	
	13. Type of Report and Period Covered
12. Sponsoring Agency Name and Address	Technical Memorandum
National Aeronautics and Space Administration Washington, DC 20546-0001	14. Sponsoring Agency Code

15. Supplementary Notes

Point of Contact: Paul J. Curran, Ames Research Center, MS 241-4, Moffett Field, CA 94035
(415) 694-3331 or FTS 464-3331

16. Abstract

To make the best use of narrowband airborne visible/infrared imaging spectrometer (AVIRIS) data, an investigator needs to know the ratio of signal to random variability or "noise" (signal-to-noise ratio or SNR). The signal is land cover dependent and varies with both wavelength and atmospheric absorption and random noise comprises sensor noise and intrapixel variability (i.e., variability within a pixel). The three existing methods for estimating the SNR are inadequate, since typical "laboratory" methods inflate while "dark current" and "image" methods deflate the SNR.

We propose a new procedure called the "geostatistical" method. It is based on the removal of periodic noise by "notch filtering" in the frequency domain and the isolation of sensor noise and intrapixel variability using the semi-variogram. This procedure was applied easily and successfully to five sets of AVIRIS data from the 1987 flying season and could be applied to remotely sensed data from broadband sensors.

17. Key Words (Suggested by Author(s))	18. Distribution Statement
Remote sensing, Semi-variogram, Imaging spectrometry, AVIRIS, Signal-to-noise ratio Spatial statistics	Unclassified-Unlimited Subject Category - 43

19. Security Classif. (of this report)	20. Security Classif. (of this page)	21. No. of pages	22. Price
Unclassified	Unclassified	24	A03

For sale by the National Technical Information Service, Springfield, Virginia 22161